



# Characterization of copper complexes with derivatives of the ligand (2-aminoethyl)bis(2-pyridylmethyl)amine (uns-penp) and their reactivity towards oxygen

Tim Brückmann<sup>a</sup>, Jonathan Becker<sup>a</sup>, Christian Würtele<sup>a</sup>, Marcel Thomas Seuffert<sup>a</sup>, Dominik Heuler<sup>a</sup>, Klaus Müller-Buschbaum<sup>a</sup>, Morten Weiß<sup>b</sup>, Siegfried Schindler<sup>a,\*</sup>

<sup>a</sup> Institut für Anorganische und Analytische Chemie, Justus-Liebig-Universität, Heinrich-Buff-Ring 17, 35392 Gießen, Germany

<sup>b</sup> Fakultät für Biologie, Chemie und Geowissenschaften, Universität Bayreuth, Universitätsstrasse 30, 95447 Bayreuth, Germany

## ARTICLE INFO

### Keywords:

Copper complex  
Tripodal ligands  
Dioxygen activation  
Peroxiso complex  
Superoxiso complex  
Stopped-flow

## ABSTRACT

A series of copper(I) complexes with ligands derived from the tripodal ligand (2-aminoethyl)bis(2-pyridylmethyl)amine (uns-penp) have been structurally characterized and their redox chemistry analyzed by cyclic voltammetry. While the redox potentials of most of the complexes were similar their reactivity towards dioxygen was quite different. While the complex with a ferrocene derived ligand of uns-penp reacted in solution at low temperatures in a two-step reaction from the preliminary formed mononuclear *end-on* superoxido complex to a quite stable dinuclear peroxido complex it did not react with dioxygen in the solid state. Other complexes also did not react with dioxygen in the solid state while some showed a reversible formation to a green compound, indicating formation of an *end-on* superoxido complex that unfortunately so far could not be characterized. In contrast, copper complexes with the Me<sub>2</sub>uns-penp and Et-iProp-uns-penp formed dinuclear peroxido complexes in a solid-state reaction. While the reaction of dioxygen with the [Cu(Me<sub>2</sub>uns-penp)]BPh<sub>4</sub> was quite slow an instant reaction took place for [Cu(Et-iProp-uns-penp)]BPh. Very unusual, it turned out that crystals of the copper(I) complex that could be structurally characterized still were crystalline when reacted with dioxygen. Therefore, it was possible to solve the structure of the corresponding dinuclear peroxido complex directly from the same batch of crystals. The crystalline structures of the copper(I) and copper(II) complex revealed that the reason for this is the fact, that the copper(I) complex is kind of preorganized for the uptake of dioxygen and does not really change in its overall structure when being oxidized.

## 1. Introduction

Copper plays an important role in organic life. Due to its accessible I/II redox pair and biological availability it is mostly present in enzymatic processes of electron transfer, dioxygen transport and oxidation/oxygenation of organic substrates [1]. During the last decades, quite some understanding had been gained for the reactions of copper(I) complexes with dioxygen and a large number of different so called “dioxygen adduct” complexes could be identified. Some structurally characterized examples of these complexes are presented in Fig. 1. Some of these complexes are found in the active site of copper enzymes, mainly monooxygenases, such as e. g. **a** (Fig. 1) in peptidylglycine  $\alpha$ -hydroxylating monooxygenase (PHM) and dopamine- $\beta$ -mono-oxygenase (D $\beta$ M) or **e** in tyrosinase. While actually, so far, only these two

species, an *end-on*  $\eta^1$ -superoxiso (**a**) and a *side-on*  $\eta^2$ : $\eta^2$ -peroxido copper complex (**e**), have been detected in biological systems, this does not mean that the other complexes in Fig. 1 are less interesting [2]. For example, bis( $\mu$ -oxido) copper complexes **f** (which in some cases can be in an equilibrium with the *side-on*  $\eta^2$ : $\eta^2$ -peroxido copper complex **e**) proved to be quite useful in selective hydroxylation reactions (only two selected examples are given in the references) [3,4]. Furthermore, we as well as Karlin and co-workers had observed that trans- $\mu$ -1,2-peroxido complexes **b** are capable to catalytically oxidize toluene selectively to benzaldehyde [5,6]. There is high interest to transfer this type of reaction from the lab into industry where such oxygenations are usually done at higher temperatures, sometimes in the presence of quite toxic chemicals and often accompanied by undesired side products. In contrast, copper complexes that model the reactivity of the natural

\* Corresponding author.

E-mail address: [siegfried.schindler@anorg.chemie.uni-giessen.de](mailto:siegfried.schindler@anorg.chemie.uni-giessen.de) (S. Schindler).

<https://doi.org/10.1016/j.jinorgbio.2021.111544>

Received 17 April 2021; Received in revised form 5 July 2021; Accepted 12 July 2021

Available online 16 July 2021

0162-0134/© 2021 Elsevier Inc. All rights reserved.

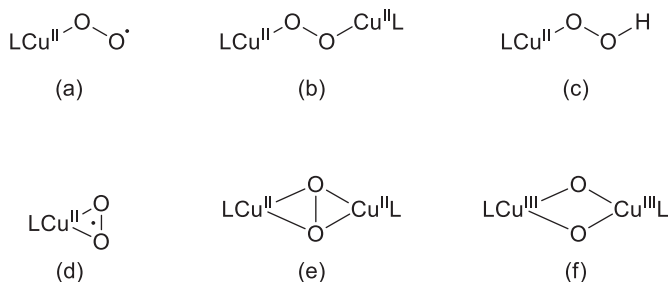
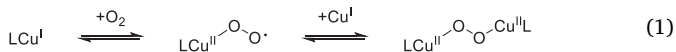


**Fig. 1.** Examples of copper “dioxygen adduct” species: (a) *end-on* superoxido, (b) *trans-μ-1,2-peroxido*, (c)  $\eta^1$ -hydroperoxido, (d) *side-on* superoxido, (e)  $\mu$ - $\eta^2$ : $\eta^2$ -peroxido, (f) *bis(μ-oxido)*.

enzymes should catalyze these reactions under ambient conditions with dioxygen from air as the sole oxidant, with high yields and with fewer side products.

The first structurally characterized “dioxygen adduct” complex, [(tmpa)Cu(O<sub>2</sub>)Cu(tmpa)](PF<sub>6</sub>)<sub>2</sub> (tmpa = tris(2-methylpyridyl)-amine, Fig. 2), a **b** system was reported by Karlin and co-workers [7]. The formation of this complex had been investigated in great detail and low temperature stopped-flow measurements allowed the brief observation of a short-lived *end-on* superoxido complex (a) in a first reaction step according to the Eq. (1) [8,9]. Due to the consecutive reaction to the dinuclear peroxido complex this labile intermediate could only be spectroscopically (UV–vis data) characterized.



Following up on these results it was possible, with the copper(I) complex and the tripodal ligand tris(2-dimethylaminoethyl)amine (Me<sub>6</sub>tren, Fig. 2), to observe the same reactivity (Eq. (1)), however here it was possible to obtain a resonance Raman spectrum of the intermediate with a characteristic peak at 1122 cm<sup>-1</sup> for the vibration frequency of <sup>16</sup>O—<sup>16</sup>O) [10].

With the tren system it seemed easy to modify the ligand system accordingly to finally stabilize an *end-on* superoxido copper enough for a full characterization. Instead, this turned out to be a journey for many years with some of the efforts by us only been published recently [11]. However, by applying the tren derivative tris(tetramethylguanidino) tren (TMG<sub>3</sub>tren, Fig. 2) as a ligand the corresponding *end-on* superoxido complex, [(TMG<sub>3</sub>tren)Cu(O<sub>2</sub>)]SbF<sub>6</sub>, was formed in a reversible reaction and was stabilized to the point that it could finally be structurally characterized [12,13]. While this complex so far is still the only example of a structurally characterized *end-on* superoxido copper complex and can be regarded as a decent model complex for PHM and DβM, it lacks their reactivity (due to the increased stability). However, most recently in a cooperation with Karlin and co-workers it could be shown that a copper(I) complex with a sulfur derivative of TMG<sub>3</sub>tren can model this reactivity [14,15].

From all these findings over the last 20 years it became clear that slight ligand modifications of the tripodal ligand system (chelate ring size, donor atoms, alkyl groups) in combination with solvent and selected anions can have a huge influence on the reaction of the

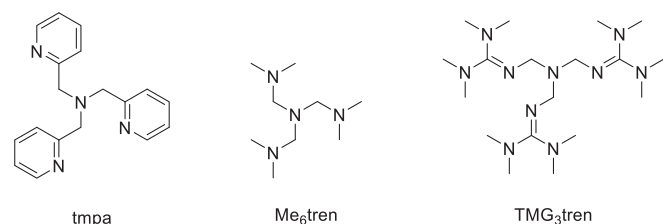


**Fig. 2.** Tripodal ligands tmpa, Me<sub>6</sub>tren and TMG<sub>3</sub>tren.

corresponding copper(I) complexes with dioxygen.

With regard to these findings we have started a thorough investigation on copper complexes with derivatives of the ligand (2-aminoethyl)bis(2-pyridylmethyl)amine (uns-penp, Fig. 3), that can be viewed as a combination of the ligands tmpa and tren. The advantage of this ligand is the possibility to easily modify the amine arm to test for the influence of different substituents or to prepare it for an immobilization [16]. To get a better picture of the influence of the amine arm modification on the reactivity of the corresponding copper(I) complexes with dioxygen we in here now present a systematic study with the ligands presented in Fig. 3.

## 2. Experimental

### 2.1. Materials and methods

All chemicals were purchased from commercial suppliers. Extra dry solvents were refluxed under argon over a drying agent prior to taking them into the glove box. [Cu(MeCN)<sub>4</sub>]<sup>+</sup> salts were synthesized according to literature methods [17]. Storage and preparation of air sensitive compounds was carried out in a glove box under an argon atmosphere (Braun, Garching, Germany; water and dioxygen <0.1 ppm). NMR measurements were performed with a Bruker Avance II 400 MHz (AV II 400) and Bruker Avance III HD 400 MHz (AV III 400). Electrospray ionization-MS (ESI-MS) measurements were performed on a Bruker microTOF mass spectrometer. UV–Vis investigations in solution were performed with an Agilent 8453 spectrometer, equipped with a cryostat CoolSpeK UV USP-203-B (Unisoku Co., Ltd., Osaka, Japan). Solid state UV–Vis spectra were recorded using a Perkin Elmer Lambda 750 UV–Vis-NIR spectrometer equipped with a Harrick praying mantis. All shown spectra were converted into absorption by the Kubelka–Munk equation [18]. A Hi-Tech SF-61SX2 low-temperature stopped-flow unit equipped with a diode array spectrophotometer (Hi-Tech, Salisbury, UK) was used for kinetic measurements in solution. A two-syringe setup was applied to perform the experiments. Detailed descriptions on the setup and the procedure have been reported previously [19]. Raman spectroscopy was executed on a SENTERRA dispersive Raman microscope (Bruker optics) equipped with a Nd:YAG laser ( $\lambda_{\text{exc}} = 532 \text{ nm}$ ). Cyclic voltammetry measurements (CV) were performed with an e-corder 410 High Resolution Laboratory Data Recorder, connected with an EA163 Potentiostat (eDAQ, Denistone East, Australia). Powder X-ray diffraction (PXRD) was carried out on a STOE STADI P diffractometer (Darmstadt, Germany), equipped with a DECTRIS MYTHEN 1 K detector and a Ge(111) monochromator. Cu K $\alpha_1$  radiation ( $\lambda = 1.5406 \text{ \AA}$ ) was used in Debye–Scherrer geometry. Samples were filled under an argon

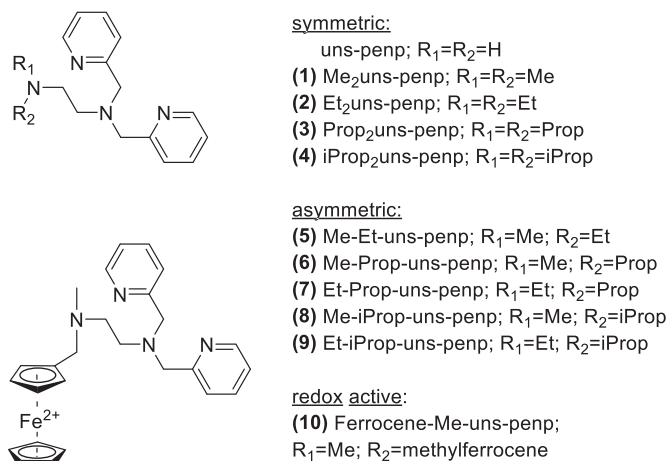


**Fig. 3.** Ligands L, derivatives of uns-penp derivatives and abbreviations (Me = methyl; Et = ethyl; Prop = propyl; iProp = isopropyl).

atmosphere into glass capillaries (Hilgenberg  $\varnothing = 0.5$  mm) and sealed prior to the measurements. The WinXPOW program package (V3.05, STOE & Cie GmbH 2011, Darmstadt, Germany) was used for data collection. Details on single crystal characterization are reported in the Supporting Information.

## 2.2. Reactivity towards oxygen

The reactions of the complexes with dioxygen were carried out either in solution or in the solid state. For reactions in solution, the complexes were dissolved in dry and dioxygen free acetone. For time resolved stopped-flow UV-Vis measurements the solutions were reacted at low temperatures with dioxygen saturated acetone. The solvent was saturated by passing dioxygen for 15 min through a syringe filled with dry acetone [20]. For other UV-Vis measurements the complex solutions were cooled to low temperatures using a cryo unit. The solutions were subsequently flushed with dioxygen. For solid state reactions, the crystalline complexes were treated with gaseous dioxygen.

## 2.3. Cyclic voltammetry measurements

The cyclic voltammetry measurements were carried out in a conventional, three-electrode setup (working, counter, and reference electrode) [21]. As working electrode, a glassy carbon electrode and as counter electrode a Pt/Ti wire were used. As reference served an Ag/AgCl electrode. The cell was prepared under an inert atmosphere. 0.1 mol/L dried tetrabutylammonium tetrafluoroborate solution in dry acetonitrile was used as electrolyte; the scanning rate was 50 mV/S. Complex concentrations of 1 mmol/L was used. During the measurements the vessel was flushed continuously with dinitrogen through a syringe to avoid air exposure.

## 2.4. Syntheses

Syntheses were performed according to procedures reported in the literature for the asymmetric uns-penp derivatives and furthermore for the basic ligand uns-penp and its derivatives [22,23].

### 2.4.1. (2-methylaminoethyl)bis(2-pyridylmethyl)amine (Me-uns-penp)

2.0 g *N*-methylthylenediamine (27.7 mmol) were dissolved in 50 mL dichloromethane (DCM). The solution was cooled to 0 °C with an ice bath and a solution of 3.83 g ethyltrifluoroacetate (27.7 mmol) in 50 mL DCM was added dropwise over a period of 40 min under argon. After the addition was complete, the resulting mixture was stirred for another 60 min at room temperature. The solvent, as well as the ethanol from the reaction were removed using a rotary evaporator. The obtained colorless oil crystallized as a white solid briefly afterwards. To attach a butoxycarbonyl (Boc) protecting group the product was dissolved in 100 mL of DCM. 5.89 g of di-*tert*-butyldicarbonate (Boc<sub>2</sub>O) in 10 mL DCM were added to the product solution at 0 °C under argon. The reaction mixture was stirred for 90 min at room temperature and then quenched with 30 mL of saturated Na<sub>2</sub>CO<sub>3</sub> solution and 30 mL of ethyl acetate. After gas formation stopped the aqueous phase was extracted three times with ethyl acetate. The combined organic layers were washed with brine, dried over MgSO<sub>4</sub>, filtrated and concentrated using a rotary evaporator. The resulting oil crystallized as a white solid after a few minutes. The product was placed into a vessel with 75 mL methanol and 25 mL of a 2–3 M NaOH solution and stirred at room temperature for two hours. Finally, methanol was removed and the aqueous layer was extracted three times with ethyl acetate. The combined organic layers were washed with brine, dried over MgSO<sub>4</sub>, filtrated and the solvent was removed under vacuum. The crude product was a pale, yellow colored oil (3.74 g, 21.5 mmol, 79%). The product was used for the following syntheses without further purification and characterization. *N,N*-Boc-methylethylenediamine was dissolved in 60 mL 1,2-dichloroethane (DCE). 4.82 g 2-pyridinecarboxaldehyde (45.1 mmol) and 13.63

sodium triacetoxyborohydride (STAB) (64.4 mmol) were added. The solution was stirred overnight under argon. Then the reaction suspension was quenched with 60 mL of 2 M NaOH solution and extracted three times with DCM. The organic layers were combined, washed with brine, dried over MgSO<sub>4</sub>, filtrated and the solvent was removed under vacuum. The resulting brown oil was treated with 100 mL half concentrated hydrochloric acid (intense gas formation was observed). The brown solution was heated to 130 °C and kept under reflux overnight. The solution was made basic by adding dropwise 6 M NaOH solution while simultaneously cooling the solution in an ice bath. The solution obtained was extracted three times with DCM, washed with brine, dried over MgSO<sub>4</sub>, filtrated and the solvent was removed under vacuum. Distillation via Kugelrohr lead to a pure product which was stored under an argon atmosphere (3.11 g, 56%). Overall yield 45% (respectively 2.0 g *N*-methylthylenediamine). <sup>1</sup>HNMR (400 MHz, CDCl<sub>3</sub>, 24 °C,  $\delta$  [ppm]): 8.53 (d, 2H, py-H), 7.65 (td, 2H, py-H); 7.48 (d, 2H, py-H), 7.14 (t, 2H, py-H), 3.85 (s, 4H, py-CH<sub>2</sub>), 2.75 (t, 2H, NCH<sub>2</sub>CH<sub>2</sub>N(CH<sub>2</sub>py)<sub>2</sub>), 2.67 (t, 2H, NCH<sub>2</sub>CH<sub>2</sub>N(CH<sub>2</sub>py)<sub>2</sub>), 2.31 (s, 2H, NCH<sub>3</sub>) <sup>13</sup>CNMR (101 MHz, CDCl<sub>3</sub>, 24 °C,  $\delta$  [ppm]): 159.6, 149.0, 136.4, 122.9, 121.9, 64.4, 60.8, 53.9, 49.4, 36.3 ESI-MS (*m/z*): [M + H]<sup>+</sup>: 257.18; [M + Na]<sup>+</sup>: 279.16

### 2.4.2. (2-ethylaminoethyl)bis(2-pyridylmethyl)amine (Et-uns-penp)

2.0 g of *N*-ethylthylenediamine (22.7 mmol) were dissolved in 50 mL DCM. The solution was cooled to 0 °C with an ice bath and a solution of 3.22 g ethyltrifluoroacetate (22.7 mmol) in 50 mL DCM was added dropwise over a period of 40 min under argon. After the addition was complete, the mixture obtained was stirred for another 60 min at room temperature. The solvent, as well as the ethanol from the reaction were removed using a rotary evaporator. The derived colorless oil crystallized as a white colored solid briefly afterwards. The product was dissolved in 100 mL of DCM. 4.95 g of Di-*tert*-butyldicarbonate in 5 mL DCM were added to the product solution at 0 °C under argon. The reaction mixture was stirred for 90 min at room temperature and then quenched with 30 mL of saturated Na<sub>2</sub>CO<sub>3</sub> solution and 30 mL of ethyl acetate. After the gas formation had stopped, the aqueous phase was extracted three times with ethyl acetate. The combined organic layers were washed with brine, dried over MgSO<sub>4</sub>, filtrated and concentrated using a rotary evaporator. The oil obtained crystallized as a white solid after a few moments. The product was placed into a vessel with 75 mL methanol and 25 mL of a 2–3 M NaOH solution and stirred at room temperature for two hours. Finally, methanol was removed and the aqueous layer was extracted three times with ethyl acetate. The combined organic layers were washed with brine, dried over MgSO<sub>4</sub>, filtrated and the solvent was removed under vacuum. The obtained crude product was a pale yellow colored oil (3.97 g, 21.1 mmol, 93%). The product was used for the following syntheses without further purification and characterization. *N,N*-Boc-ethylthylenediamine was dissolved in 60 mL DCE. 4.52 g 2-pyridinecarboxaldehyde (42.2 mmol) and 13.41 STAB (63.3 mmol) were added. The solution was stirred overnight under argon. Then the reaction suspension was quenched with 60 mL of 2 M NaOH solution and extracted three times with DCM. The organic layers were combined, washed with brine, dried over MgSO<sub>4</sub>, and after filtration the solvent was removed under vacuum. The obtained brown colored oil was treated with 100 mL half concentrated hydrochloric acid (intense gas formation was observed). The brown solution was heated to 130 °C and refluxed overnight. The solution was made basic by adding dropwise 6 M NaOH solution by simultaneous cooling it in an ice bath. The resulting solution was extracted three times with DCM, washed with brine, dried over MgSO<sub>4</sub>, filtrated and the solvent was removed under vacuum. Distillation via Kugelrohr lead to a pure product which was stored under an argon atmosphere (3.49 g, 61%). Overall yield 57% (in respect to starting material *N*-ethylthylenediamine). <sup>1</sup>HNMR (400 MHz, CDCl<sub>3</sub>, 23 °C,  $\delta$  [ppm]): 8.48 (d, 2H, py-H), 7.60 (td, 2H, py-H), 7.43 (d, 2H, py-H), 7.09 (t, 2H, py-H), 3.81 (s, 4H, py-CH<sub>2</sub>), 2.75–2.62 (m, 4H, NCH<sub>2</sub>CH<sub>2</sub>N), 2.45 (q, 2H, NCH<sub>2</sub>CH<sub>3</sub>), 1.00 (t, 3H, NCH<sub>2</sub>CH<sub>3</sub>). <sup>13</sup>CNMR (101 MHz, CDCl<sub>3</sub>, 24 °C,  $\delta$  [ppm]):  $\delta$  159.7, 149.0, 148.5, 136.5, 136.4,

122.9, 122.1, 121.9, 120.4, 64.3, 60.8, 54.2, 47.1, 44.0, 15.3. **ESI-MS** ( $m/z$ ):  $[M + H]^+$ : 271.19;  $[M + Na]^+$ : 293.17

**2.4.2.1. Symmetric uns-penp derivatives.** The preparation of symmetric uns-penp derivatives Me<sub>2</sub>uns-penp and Et<sub>2</sub>uns-penp were reported previously [24,25]. Furthermore, the synthesis of the ligand iProp<sub>2</sub>uns-penp was performed according to these descriptions. The ligand Prop<sub>2</sub>uns-penp was synthesized from uns-penp. The terminal primary amine was subsequently modified via an S<sub>N</sub>2 reaction [23,26].

#### 2.4.3. Me<sub>2</sub>uns-penp (1)

*N,N*-dimethylethylenediamine (2.0 g, 22.7 mmol) was dissolved in 30 mL of DCE. 2-pyridincarboxaldehyde (4.86 g; 45.4 mmol) and STAB (14.43 g; 68.1 mmol) were added. The foamy mixture was stirred at room temperature overnight under an argon atmosphere. The reaction was quenched with 30 mL of 2 M NaOH solution and extracted three times with DCM. The combined organic layers were washed with brine and dried over MgSO<sub>4</sub>. The crude product was obtained by removing the solvent. The pure product was obtained by purification via Kugelrohr distillation. The light brown colored oil was stored under an argon atmosphere (4.83 g, 79%). <sup>1</sup>H NMR (400 MHz, CDCl<sub>3</sub>, 26 °C, δ [ppm]): 8.48 (d, 2H, py-H), 7.60 (td, 2H, py-H), 7.49 (d, 2H, py-H), 7.09 (t, 2H, py-H), 3.82 (s, 4H, py-CH<sub>2</sub>), 2.69–2.63 (t, 2H, NCH<sub>2</sub>CH<sub>2</sub>N(CH<sub>2</sub>py)<sub>2</sub>), 2.45 (t, 2H, NCH<sub>2</sub>CH<sub>2</sub>N(CH<sub>2</sub>py)<sub>2</sub>), 2.13 (s, 6H, N(CH<sub>3</sub>)<sub>2</sub>). <sup>13</sup>C NMR (101 MHz, CDCl<sub>3</sub>, 28 °C, δ [ppm]): 149.8, 149.2, 149.0, 136.9, 136.7, 136.3, 122.9, 122.4, 122.3, 122.2, 121.9, 120.4, 60.53, 45.8, 45.61, 5.5, 21.8. **ESI-MS** ( $m/z$ ):  $[M + H]^+$ : 270.18.

#### 2.4.4. Et<sub>2</sub>uns-penp (2)

*N,N*-diethylethylenediamine (2.0 g, 17.2 mmol) was dissolved in 30 mL of DCE. 2-pyridincarboxaldehyde (3.69 g; 34.4 mmol) and STAB (10.94 g; 51.6 mmol) were added. The foamy mixture was stirred at room temperature overnight under argon. The reaction was quenched with 30 mL of 2 M NaOH solution and extracted three times with DCM. The combined organic layers were washed with brine and dried over MgSO<sub>4</sub>. The crude product was obtained by removing the solvent. The pure product was obtained by purification via Kugelrohr distillation. The light brown colored oil was stored under an argon atmosphere (3.04 g, 59%). <sup>1</sup>H NMR (400 MHz, CDCl<sub>3</sub>, 26 °C, δ [ppm]): 8.50 (d, 2H, py-H), 7.62 (td, 2H, py-H), 7.53 (d, 2H, py-H), 7.11 (t, 2H, py-H), 3.85 (s, 4H, py-CH<sub>2</sub>), 2.67 (t, 2H, NCH<sub>2</sub>CH<sub>2</sub>N(CH<sub>2</sub>py)<sub>2</sub>), 2.60 (t, 2H, NCH<sub>2</sub>CH<sub>2</sub>N(CH<sub>2</sub>py)<sub>2</sub>), 2.44 (q, 4H, N(CH<sub>2</sub>CH<sub>3</sub>)<sub>2</sub>), 0.93 (t, 6H, N(CH<sub>2</sub>CH<sub>3</sub>)<sub>2</sub>). <sup>13</sup>C NMR (101 MHz, CDCl<sub>3</sub>, 26 °C, δ [ppm]): 160.0, 149.0, 136.3, 122.8, 121.9, 61.0, 52.3, 50.9, 47.5, 47.4, 11.8. **ESI-MS** ( $m/z$ ):  $[M + H]^+$ : 298.22.

#### 2.4.5. Prop<sub>2</sub>uns-penp (3)

The precursor ligand uns-penp was synthesized according to the literature and purified via Kugelrohr distillation [23]. The such purified uns-penp (1.0 g; 4.1 mmol) was dissolved in 20 mL acetonitrile. K<sub>2</sub>CO<sub>3</sub> (4.1 g; 30.0 mmol) and 1-iodopropane (1.50 g; 8.8 mmol) were added to the solution. The mixture was stirred overnight at 50 °C under an argon atmosphere. Afterwards the solvent was removed. The residue was treated with diethylether, filtrated and the solvent was removed. Kugelrohr distillation led to a pure product that was stored under an argon atmosphere (0.90 g; 67%). <sup>1</sup>H NMR (400 MHz, CDCl<sub>3</sub>, 24 °C, δ [ppm]): 8.48 (d, 2H, py-H), 7.61 (td, 2H, py-H), 7.52 (d, 2H, py-H), 7.10 (t, 2H, py-H), 3.83 (s, 4H, py-CH<sub>2</sub>), 2.61 (m, 4H, NCH<sub>2</sub>CH<sub>2</sub>N), 2.27 (t, 4H, N(CH<sub>2</sub>CH<sub>2</sub>CH<sub>3</sub>)<sub>2</sub>), 1.34 (m, 4H, N(CH<sub>2</sub>CH<sub>2</sub>CH<sub>3</sub>)<sub>2</sub>), 0.77 (t, 6H, N(CH<sub>2</sub>CH<sub>2</sub>CH<sub>3</sub>)<sub>2</sub>). <sup>13</sup>C NMR (101 MHz, CDCl<sub>3</sub>, 27 °C, δ [ppm]): 160.1, 149.1, 136.4, 122.9, 121.9, 61.1, 56.8, 52.4, 20.4, 12.0. **ESI-MS** ( $m/z$ ):  $[M + H]^+$ : 327.26;  $[M + Na]^+$ : 349.24.

#### 2.4.6. iProp<sub>2</sub>uns-penp (4)

*N,N*-diisopropylethylenediamine (1.0 g, 6.9 mmol) was dissolved in

50 mL DCE. 2-pyridincarboxaldehyde (1.48 g; 13.8 mmol) and STAB (4.41 g; 20.8 mmol) were added. The foamy mixture was stirred at room temperature overnight under argon. The reaction was quenched with 50 mL of 2 M NaOH solution and extracted three times with DCM. The combined organic layers were washed with brine and dried over MgSO<sub>4</sub>. The crude product was obtained by removing the solvent. The pure product was obtained by purification via Kugelrohr distillation. The light brown colored oil was stored under an argon atmosphere (1.63 g, 72%). <sup>1</sup>H NMR (400 MHz, CDCl<sub>3</sub>, 23 °C, δ [ppm]): 8.50 (d, 2H, py-H), 7.62 (td, 2H, py-H), 7.56 (d, 2H, py-H), 7.11 (t, 2H, py-H), 3.84 (s, 4H, py-CH<sub>2</sub>), 2.88 (m, 4H, NCH(CH<sub>3</sub>)<sub>2</sub>), 2.55 (s, 4H, NCH<sub>2</sub>CH<sub>2</sub>N), 0.89 (d, 12H, NCH(CH<sub>3</sub>)<sub>2</sub>). <sup>13</sup>C NMR (101 MHz, CDCl<sub>3</sub>, 24 °C, δ [ppm]): 160.2, 149.0, 136.3, 122.7, 121.8, 61.1, 56.4, 49.1, 43.6, 20.6. **ESI-MS** ( $m/z$ ):  $[M + H]^+$ : 327.26;  $[M + Na]^+$ : 349.24.

**2.4.6.1. Asymmetric uns-penp derivatives.** The asymmetric ligands are based on the priorly synthesized precursor ligands with a secondary amine at the terminal position. The second alkyl residue was added via a simple S<sub>N</sub>2 reaction in an established procedure [26]. However, the Ferrocene residue was connected via reductive alkylation [23].

#### 2.4.7. Me-Et-uns-penp (5)

Me-uns-penp (1.0 g, 3.9 mmol) was dissolved in 20 mL acetonitrile. Bromoethane (0.74 g; 6.8 mmol) and K<sub>2</sub>CO<sub>3</sub> (2.5 g; 18.1 mmol) were added. The solution was stirred at 50 °C under argon for three days. The solvent was removed. The residue was treated with diethyl ether, and the solvent was removed after filtration. Kugelrohr distillation led to a pure product that was stored under an argon atmosphere (0.60 g; 54%). <sup>1</sup>H NMR (400 MHz, CDCl<sub>3</sub>, 23 °C, δ [ppm]): 8.49 (d, 2H, py-H), 7.61 (td, 2H, py-H), 7.52 (d, 2H, py-H), 7.10 (t, 2H, py-H), 3.83 (s, 4H, py-CH<sub>2</sub>), 2.68 (t, 2H, NCH<sub>2</sub>CH<sub>2</sub>N(CH<sub>2</sub>py)<sub>2</sub>), 2.52 (t, 2H, NCH<sub>2</sub>CH<sub>2</sub>N(CH<sub>2</sub>py)<sub>2</sub>), 2.33 (q, 2H, NCH<sub>2</sub>CH<sub>3</sub>), 2.12 (s, 3H, NCH<sub>3</sub>), 0.97 (t, 3H, NCH<sub>2</sub>CH<sub>3</sub>). <sup>13</sup>C NMR (101 MHz, CDCl<sub>3</sub>, 25 °C, δ [ppm]): 160.0, 149.1, 136.4, 123.0, 122.0, 61.0, 55.2, 52.3, 51.8, 42.1, 12.3. **ESI-MS** ( $m/z$ ):  $[M + H]^+$ : 285.21;  $[M + Na]^+$ : 307.19.

#### 2.4.8. Me-Prop-uns-penp (6)

Me-uns-penp (1.0 g, 3.9 mmol) was dissolved in 20 mL acetonitrile. 1-iodopropane (0.70 g; 4.1 mmol) and K<sub>2</sub>CO<sub>3</sub> (2.5 g; 18.1 mmol) were added. The solution was stirred at 50 °C under argon for two days. The solvent was removed. The residue was treated with diethyl ether, filtrated and the solvent was removed. Kugelrohr distillation led to a pure product that was stored under an argon atmosphere (0.65 g; 56%). <sup>1</sup>H NMR (400 MHz, CDCl<sub>3</sub>, 23 °C, δ [ppm]): 8.49 (d, 2H, py-H), 7.61 (td, 2H, py-H), 7.52 (d, 2H, py-H), 7.10 (t, 2H, py-H), 3.83 (s, 4H, py-CH<sub>2</sub>), 2.67 (t, 2H, NCH<sub>2</sub>CH<sub>2</sub>N(CH<sub>2</sub>py)<sub>2</sub>), 2.52 (t, 2H, NCH<sub>2</sub>CH<sub>2</sub>N(CH<sub>2</sub>py)<sub>2</sub>), 2.21 (t, 2H, NCH<sub>2</sub>CH<sub>2</sub>CH<sub>3</sub>), 2.14 (s, 3H, NCH<sub>3</sub>), 1.40 (h, 2H, NCH<sub>2</sub>CH<sub>2</sub>CH<sub>3</sub>), 0.80 (t, 2H, NCH<sub>2</sub>CH<sub>2</sub>CH<sub>3</sub>). <sup>13</sup>C NMR (101 MHz, CDCl<sub>3</sub>, 24 °C, δ [ppm]): 160.0, 149.1, 136.41, 122.9, 122.0, 61.0, 60.2, 55.7, 52.3, 42.7, 20.5, 12.0. **ESI-MS** ( $m/z$ ):  $[M + H]^+$ : 299.22.

#### 2.4.9. Et-Prop-uns-penp (7)

Et-uns-penp (1.0 g, 3.7 mmol) was dissolved in 20 mL acetonitrile. 1-iodopropane (0.87 g; 5.1 mmol) and K<sub>2</sub>CO<sub>3</sub> (2.5 g; 18.1 mmol) were added. The solution was stirred at 50 °C under an argon atmosphere for seven days. The solvent was removed. The residue was treated with diethyl ether, filtrated and the solvent was removed. Kugelrohr distillation led to a pure product that was stored under an argon atmosphere (0.75 g; 65%). <sup>1</sup>H NMR (400 MHz, CDCl<sub>3</sub>, 23 °C, δ [ppm]): 8.49 (d, 2H, py-H), 7.62 (td, 2H, py-H), 7.53 (d, 2H, py-H), 7.10 (t, 2H, py-H), 3.84 (s, 4H, py-CH<sub>2</sub>), 2.62 (m, 4H, NCH<sub>2</sub>CH<sub>2</sub>N), 2.42 (q, 2H, NCH<sub>2</sub>CH<sub>3</sub>), 2.28 (t, 2H, NCH<sub>2</sub>CH<sub>2</sub>CH<sub>3</sub>), 1.36 (h, 2H, NCH<sub>2</sub>CH<sub>2</sub>CH<sub>3</sub>), 0.80 (t, 2H, NCH<sub>2</sub>CH<sub>2</sub>CH<sub>3</sub>), 0.92 (t, 3H, NCH<sub>2</sub>CH<sub>3</sub>), 0.78 (t, 3H, NCH<sub>2</sub>CH<sub>2</sub>CH<sub>3</sub>). <sup>13</sup>C NMR (101 MHz, CDCl<sub>3</sub>, 26 °C, δ [ppm]): 160.1, 149.1, 136.4, 122.9, 121.9, 61.1, 56.13, 52.4, 51.7, 48.1, 20.4, 12.0, 11.9. **ESI-MS** ( $m/z$ ):  $[M$

+ H]<sup>+</sup>: 313.24, [M + Na]<sup>+</sup>: 335.22.

#### 2.4.10. Me-iProp-uns-penp (8)

Me-uns-penp (0.71 g, 2.8 mmol) was dissolved in 20 mL acetonitrile. 2-iodopropane (0.75 g; 4.4 mmol) and K<sub>2</sub>CO<sub>3</sub> (2.5 g; 18.1 mmol) were added. The solution was stirred at 50 °C under argon for four days. The solvent was removed. The residue was treated with diethylether, filtrated and the solvent was removed. Kugelrohr distillation led to a pure product that was stored under an argon atmosphere (0.51 g; 62%). <sup>1</sup>H NMR (400 MHz, CDCl<sub>3</sub>, 25 °C, δ [ppm]): 8.49 (d, 2H, py-H), 7.61 (td, 2H, py-H), 7.53 (d, 2H, py-H), 7.09 (t, 2H, py-H), 3.84 (s, 4H, py-CH<sub>2</sub>), 2.72 (h, 1H, NCH(CH<sub>3</sub>)<sub>2</sub>), 2.65 (t, 2H, NCH<sub>2</sub>CH<sub>2</sub>N(CH<sub>2</sub>py)<sub>2</sub>), 2.53 (t, 2H, NCH<sub>2</sub>CH<sub>2</sub>N(CH<sub>2</sub>py)<sub>2</sub>), 2.10 (s, 3H, NCH<sub>3</sub>), 0.91 (d, 2H, NCH(CH<sub>3</sub>)<sub>2</sub>). <sup>13</sup>C NMR (101 MHz, CDCl<sub>3</sub>, 26 °C, δ [ppm]): 160.1, 149.1, 136.4, 122.9, 121.9, 61.0, 53.8, 53.1, 51.3, 37.5, 18.0. ESI-MS (m/z): [M + H]<sup>+</sup>: 299.22, [M + Na]<sup>+</sup>: 321.21.

#### 2.4.11. Et-iProp-uns-penp (9)

Et-uns-penp (1.0 g, 3.7 mmol) was dissolved in 20 mL acetonitrile. 2-iodopropane (1.74 g; 10.2 mmol) and K<sub>2</sub>CO<sub>3</sub> (5.0 g; 36.2 mmol) were added. The solution was refluxed under argon for five days. The solvent was removed. The residue was treated with diethyl ether, filtrated and the solvent was removed. Kugelrohr distillation led to a pure product that was stored under an argon atmosphere (0.77 g; 67%). <sup>1</sup>H NMR (400 MHz, CDCl<sub>3</sub>, 23 °C, δ [ppm]): 8.49 (d, 2H, py-H), 7.62 (td, 2H, py-H), 7.54 (d, 2H, py-H), 7.10 (t, 2H, py-H), 3.84 (s, 4H, py-CH<sub>2</sub>), 2.84 (h, 1H, NCH(CH<sub>3</sub>)<sub>2</sub>), 2.61 (t, 2H, NCH<sub>2</sub>CH<sub>2</sub>N(Py)<sub>2</sub>), 2.54 (t, 2H, NCH<sub>2</sub>CH<sub>2</sub>N(Py)<sub>2</sub>), 2.38 (q, 2H, NCH<sub>2</sub>CH<sub>3</sub>), 0.90 (m, 9H, NCH<sub>2</sub>CH<sub>3</sub> and NCH(CH<sub>3</sub>)<sub>2</sub>). <sup>13</sup>C NMR (101 MHz, CDCl<sub>3</sub>, 23 °C, δ [ppm]): 160.1, 149.3, 149.1, 136.4, 122.9, 121.9, 61.1, 54.4, 50.8, 47.6, 44.9, 18.4, 14.1. ESI-MS (m/z): [M + H]<sup>+</sup>: 313.24, [M + Na]<sup>+</sup>: 335.22.

#### 2.4.12. Ferrocene-Me-uns-penp (10)

Me-uns-penp (0.50 g; 2.0 mmol) was dissolved in 20 mL DCE. Ferrocene aldehyde (0.46 g; 2.1 mmol) and STAB (0.94 g; 4.4 mmol) were added. The reaction mixture was stirred at room temperature under argon atmosphere overnight. The reaction was quenched with 30 mL of 2 M NaOH and extracted with DCM. The combined organic layers were washed with brine, dried over MgSO<sub>4</sub> and the solvent was removed. The product was purified by column chromatography on silica as stationary phase eluted with DCM/MeOH (95: 5 v/v, + 0,2 vol% DIPEA). The solvent of the collected fractions was removed and the obtained oil was transferred into a glove box. Subsequently the crude product was dissolved in dry diethylether and treated with a small amount of DIPEA. After stirring for a few minutes, the solution was separated via a syringe filter (0.2 μm) and the solvent and the residual DIPEA as well were removed under vacuum. ESI-MS (m/z): [M + H]<sup>+</sup>: 455.19.

Copper(I) complexes: All copper(I) complexes with tetraphenylborate as anion were obtained under inert conditions according to a general procedure described in the literature [5]. In case of [Cu(10)]BPh<sub>4</sub>, the copper(I) salt [Cu(MeCN)<sub>4</sub>]SO<sub>3</sub>CF<sub>3</sub> was used to prevent disproportionation.

#### 2.4.13. [Cu(Ligand)]BPh<sub>4</sub>

200 mg of the ligand were dissolved in a small amount of dry acetone. A solution of 0.95 eq [Cu(MeCN)<sub>4</sub>]PF<sub>6</sub> was dissolved in a small amount of dry acetone and added dropwise to the ligand solution while stirring. Afterwards, 1.05 eq NaBPh<sub>4</sub> was added. The complex was precipitated by dropwise addition into dry diethyl ether. The yellow solid was filtrated, washed with diethyl ether and dried under vacuum. Diffusion of diethyl ether led to crystals which were suitable for X-ray analysis (except for [Cu(iProp<sub>2</sub>uns-penp)]BPh<sub>4</sub>, detection via ESI-MS).

Copper(II) complexes: All copper(II) complexes with coordinating chloride and non-coordinating perchlorate as anion were obtained according to a general procedure described in the literature [23].

#### 2.4.14. [Cu(Ligand)Cl]ClO<sub>4</sub>

70 mg of the ligand was dissolved in 2 mL of methanol. A solution of 0.5 eq of copper(II)chloride dehydrate and 0.5 eq copper(II)perchlorate hexahydrate were dissolved in 4 mL of methanol. The blue solution containing the copper salts was added to the ligand solution. Slow evaporation yielded crystals suitable for X-ray analysis.

### 3. Results and discussion

#### 3.1. Syntheses and characterization

The ligands presented in Fig. 3 were synthesized without too many problems in acceptable yields according to published procedures. Symmetrical ligands Me<sub>2</sub>uns-penp, Et<sub>2</sub>uns-penp and iProp<sub>2</sub>uns-penp could be obtained from commercially available chemicals in a one step-reaction. Only for the synthesis of ligand Prop<sub>2</sub>uns-penp, uns-penp was needed as a precursor. The addition of the second alkyl residue for the unsymmetric ligands was performed under basic conditions in a S<sub>N</sub>2 reaction. The reaction duration of the synthesis of Et-iProp-uns-penp was striking. A reason for this might be the strong steric hindrance around the fully substituted nitrogen atom. This effect further explains the lack of an oversubstitution which was detected within all other S<sub>N</sub>2 reactions performed. All ligands needed to be purified by Kugelrohr distillation. Ferrocene aldehyde was attached to the Me-uns-penp ligand by reductive alkylation. Here purification via Kugelrohr distillation was not possible due to similar sublimation temperatures of the final ligand and the reactants. However, with column chromatography separation was achieved and after a final treatment with base under inert conditions the pure ligand was obtained.

The copper(I) complexes had to be synthesized under inert conditions in a glove box (argon) due to their high sensitivity towards air and moisture. However, it was possible to determine the molecular structures by SCXRD of the copper(I) complexes with all ligands in Fig. 3 with the exception of the copper(I) complex with iProp<sub>2</sub>uns-penp as a ligand. Therefore, [Cu(4)]BPh<sub>4</sub> was analyzed by ESI-MS instead. While molecular structures of [Cu(1)]BPh<sub>4</sub> and [Cu(6)]BPh<sub>4</sub> have been reported previously crystallographic data for [Cu(1)]BPh<sub>4</sub> have not been published yet (crystallographic data are reported in the Supporting Information, Tables SI-5 – SI-9) [16,27]. As an example for a copper(I) complex with a symmetric ligand arm, Fig. 4 shows the molecular structure of the cation of [Cu(1)]BPh<sub>4</sub> with its symmetry equivalent. As an example for a copper(I) complex with an asymmetric ligand arm, the molecular structure of the cation of [Cu(9)]BPh<sub>4</sub> (one complex cation and its symmetry equivalent to show their relative orientation) is

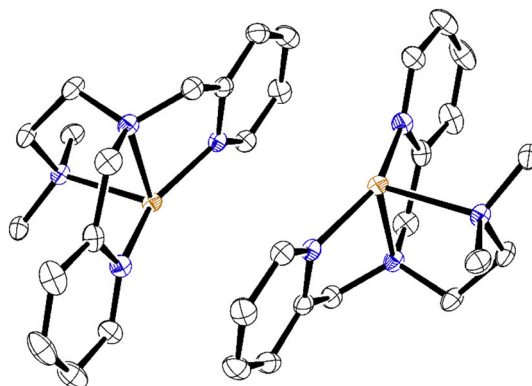


Fig. 4. Molecular structure of the cation of [Cu(1)]BPh<sub>4</sub> complex and its symmetry equivalent (–x, 1-y, 1-z). Ellipsoids set at 50% probability; the anions, H atoms, and solvent molecules are omitted for clarity. Carbon: black; nitrogen: blue; copper: brown. (For interpretation of the references to color in this figure legend, the reader is referred to the web version of this article.)

presented in Fig. 5. Furthermore, the molecular structure of the cation of the somewhat a bit more special copper(I) complex with the redox active ferrocene derivative as ligand, [Cu(10)]BPh<sub>4</sub> is shown in Fig. 6. The molecular structures of all copper(I) complexes as well as their crystallographic data are reported in the Supporting Information (Figs. SI-8 – SI-15 and Tables SI-5 – SI-44). These complexes are perfectly in line with the data already reported for related copper(I) complexes with tripodal ligands [19,28,29].

Due to the fact that usually “dioxygen adduct” copper complexes are only spectroscopically observed as reactive intermediates, molecular structures of these compounds are rare. However, to get an idea for the structure of these complexes, it is a good strategy to structurally characterize the corresponding copper(II) complexes with chloride anions as additional ligands (representing/modelling the binding of the oxygen atom) [28–30]. Copper(II) complexes with chloride could be structurally characterized and molecular structures of the cations of [Cu(2)Cl]ClO<sub>4</sub>, [Cu(3)Cl]ClO<sub>4</sub>, [Cu(5)Cl]ClO<sub>4</sub>, [Cu(7)Cl]ClO<sub>4</sub>, [Cu(8)Cl]ClO<sub>4</sub> and [Cu(9)Cl]ClO<sub>4</sub> as well as crystallographic data are reported in the Supporting Information (Figs. SI-16 – SI-22 and Tables SI-45 – SI-81). The molecular structure of [Cu(6)Cl]ClO<sub>4</sub> has been reported previously [16]. No crystals suitable for structural characterization of the copper(II) complex with the Ferrocene-Me-uns-penp (10) were obtained. Furthermore, efforts to crystallize and structurally characterize [Cu(4)Cl]ClO<sub>4</sub> were not successful. Instead, crystallization of the product from a solution of this complex showed that the (iProp)<sub>2</sub>-amine group obviously got detached from the ligand and that the remaining ligand part was oxidized. The molecular structure of this complex [Cu(11)Cl] (11 = dipicolinamide anion) is presented in the Supporting Information (Fig. SI-1). The molecular structure has already been reported previously [31,32]. While the mechanism of this reaction is not completely clear yet, it is more than likely that it follows a similar mechanism proposed for related copper complexes [33,34]. The reactivity of copper chloride towards organic substrates is beyond the scope of this work and was not investigated any further herein.

### 3.2. Cyclic voltammetry

To gain more information on the influence of the alternating residues at the terminal amine with regard to their redox potentials, cyclic voltammetry was performed in acetonitrile. The cyclic voltammograms for symmetric and asymmetric substituted ligands are shown in Figs. 7 and 8. The redox potentials are reported in Table 1. All complexes show a reversible Cu(I)/Cu(II) redox reaction and the potentials of nearly all copper(I) complexes are quite similar with a value of  $E_{1/2}$  close to 0.1 V.

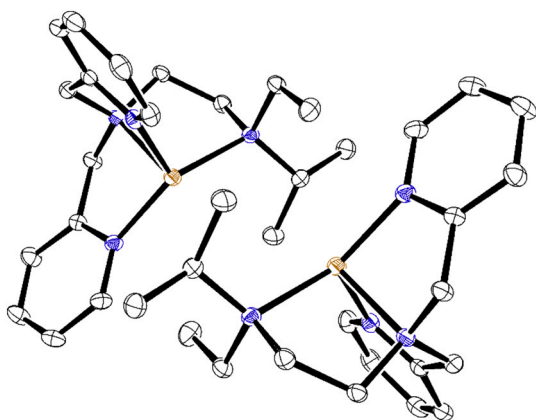


Fig. 5. Molecular structure of the cation of [Cu(9)]BPh<sub>4</sub> complex and its symmetry equivalent (2-x, 2-y, 1-z). Ellipsoids set at 50% probability; the anions, H atoms, and solvent molecules are omitted for clarity. Carbon: black; nitrogen: blue; copper: brown. (For interpretation of the references to color in this figure legend, the reader is referred to the web version of this article.)

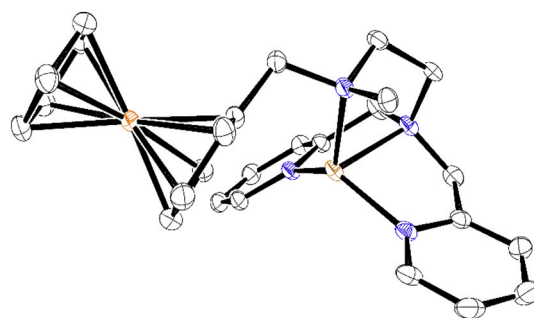


Fig. 6. Molecular structure of the cation of [Cu(10)]BPh<sub>4</sub> complex. Ellipsoids set at 50% probability; the anions, H atoms, and solvent molecules are omitted for clarity. Carbon: black; nitrogen: blue; iron: orange; copper: brown. (For interpretation of the references to color in this figure legend, the reader is referred to the web version of this article.)

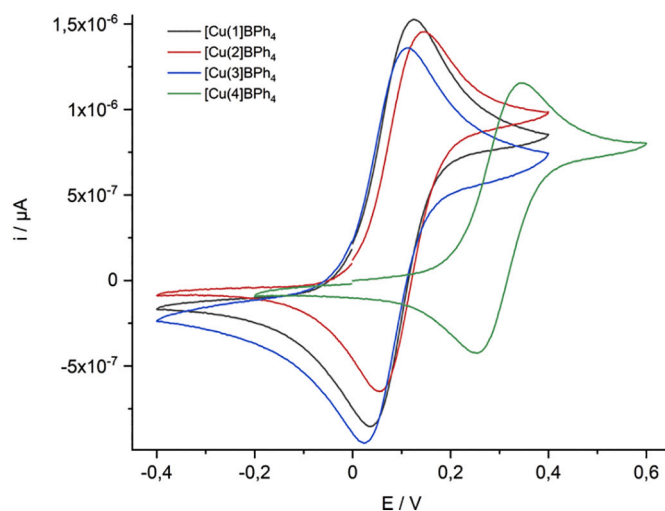


Fig. 7. Cyclic voltammograms of the copper(I) complexes with ligands 1, 2, 3 and 4 (symmetric uns-penp derivatives) in acetonitrile at room temperature. [complex] = 1 mmol/L; [electrolyte] ([NBu<sub>4</sub>]BF<sub>4</sub>) = 0.1 mol/L.

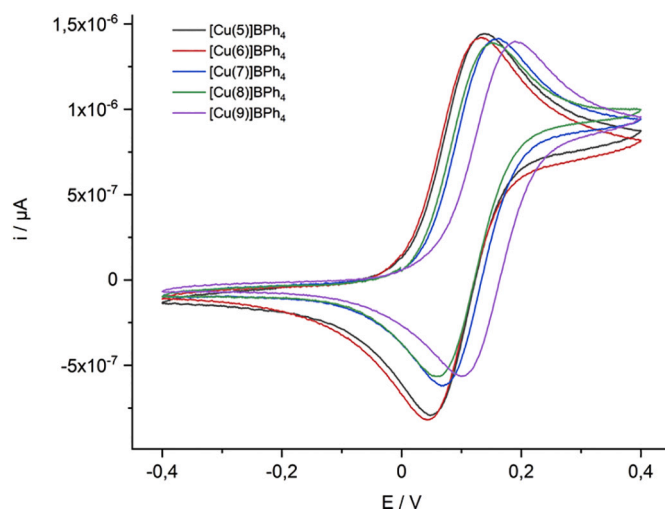


Fig. 8. Cyclic voltammograms of the copper(I) complexes with ligands 5, 6, 7, 8 and 9 (asymmetric uns-penp derivatives) in acetonitrile at room temperature. [complex] = 1 mmol/L; [electrolyte] ([NBu<sub>4</sub>]BF<sub>4</sub>) = 0.1 mol/L.

**Table 1**  
Potentials of the copper(I) complexes and ferrocene in comparison.

	$E_p^{red}$ [V]	$E_p^{ox}$ [V]	$E_{1/2}$ [V]	$\Delta E$ [mV]
[Cu(1)]BPh <sub>4</sub>	0.034	0.127	0.081	93
[Cu(2)]BPh <sub>4</sub>	0.055	0.147	0.101	92
[Cu(3)]BPh <sub>4</sub>	0.023	0.115	0.069	92
[Cu(4)]BPh <sub>4</sub>	0.254	0.348	0.301	94
[Cu(5)]BPh <sub>4</sub>	0.048	0.140	0.094	92
[Cu(6)]BPh <sub>4</sub>	0.043	0.132	0.088	89
[Cu(7)]BPh <sub>4</sub>	0.066	0.163	0.115	97
[Cu(8)]BPh <sub>4</sub>	0.059	0.152	0.106	93
[Cu(9)]BPh <sub>4</sub>	0.100	0.189	0.145	89
[Cu(10)]BPh <sub>4</sub>	0.014	0.130	0.072	116
	0.848	0.930	0.889	82
		1.270		
ferrocene	0.613	0.686	0.650	73

Not unexpected, [Cu(4)]BPh<sub>4</sub> has a much higher potential with  $E_{1/2} = 0.301$  V. Furthermore, the potential  $E_{1/2} = 0.145$  V of [Cu(9)]BPh<sub>4</sub> is somewhat higher with regard to the other complexes. This can be easily explained by the known fact that the *N*-donor atom can dissociate from the metal ion in the tripodal complex if the *R* groups become sterically too demanding. Acetonitrile that has been used for the CV measurements is a strongly competing ligand that additionally will enforce such a dissociation. So the CV of [Cu(4)]BPh<sub>4</sub> most likely shows the redox potential of the complex [Cu(4)(CH<sub>3</sub>CN)<sub>x</sub>]BPh<sub>4</sub> with a detached amine arm and therefore is quite different in comparison with the other complexes.

Complex [Cu(10)]BPh<sub>4</sub> was synthesized to integrate an internal redox indicator. It is treated separately because the modification of the uns-penp ligand is much bigger in comparison with the other ligands applied. The CV of this complex is presented in Fig. 9 and potentials are reported in Table 1. The redox potential of the copper complex is well in line with the other complexes and does not seem to be influenced by the directly bonded ferrocene unit. The potential of the ferrocene unit with 0.89 V is shifted to a more positive value compared with 0.65 V of the free ferrocene under these conditions. However, this again is expected because ferrocene derivatives such as ferrocene aldehyde show similar shifts in comparison with ferrocene [35].

### 3.3. Reactivity towards dioxygen

The reactivity of the copper(I) complexes with uns-penp and Me<sub>2</sub>uns-penp (**1**) towards dioxygen have been studied in great detail in the same way as with the ligands tmpa and Me<sub>6</sub>tren [9,10,19,23,36]. As described

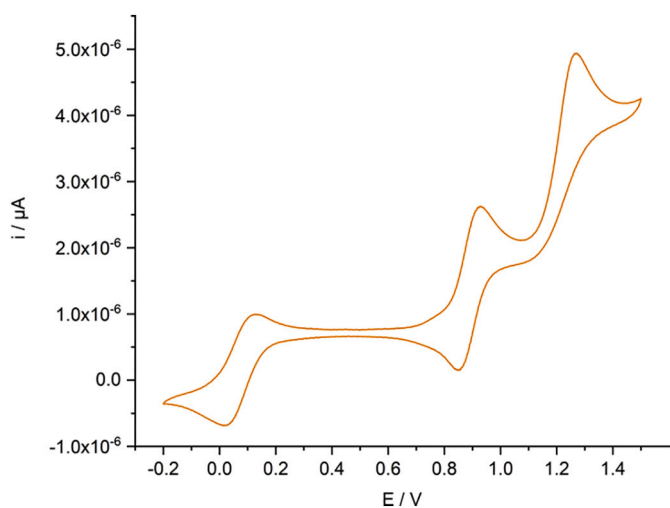


**Fig. 9.** Cyclic voltammogram of [Cu(10)]BPh<sub>4</sub> in acetonitrile at room temperature. [complex] = 1 mmol/L; [electrolyte] ([NBu<sub>4</sub>]BF<sub>4</sub>) = 0.1 mol/L.

in the introduction these complexes form quite stable trans- $\mu$ -1,2,-peroxido copper complexes at low temperatures (Eq. (1)). The same behavior was observed for the copper complexes with ligands **2**, **3** and **5–10**. The UV–vis spectra of [Cu(1)]BPh<sub>4</sub>, [Cu(4)]BPh<sub>4</sub> and [Cu(9)]BPh<sub>4</sub> prior and after their reaction with dioxygen in acetone at  $-85$  °C are presented in Fig. 10. The typical spectra of the dinuclear copper peroxido complexes with an absorbance maximum at around 530 nm and a shoulder around 600 nm are observed [37,38]. The UV–vis spectra of the other copper dioxygen “adduct” complexes are reported in the Supporting Information (Figs. SI-2 and SI-3).

Again, [Cu(4)]BPh<sub>4</sub> shows different reactivity, as can be seen in Fig. 10. Only a small and very broad maximum was observed that could be assigned to the corresponding trans- $\mu$ -1,2,-peroxido copper complex, indicating an already decaying oxygen “adduct complex”. Time resolved UV–Vis spectra obtained in a stopped-flow measurement at  $-83$  °C in acetone (Fig. 11) revealed a fast formation of the peroxido complex within 1.7 s at 550 nm according to Eq. (1) (briefly the superoxido intermediate can be seen as well with an absorbance maximum at 420 nm). Despite the low temperature, the peroxido complex is not stable and decomposes over two minutes (time trace shown in the inset in Fig. 11). This furthermore explains the observation from Fig. 10 and gives a hint towards the decomposition and oxidation of **4** described above.

Quite surprising was the fact that the copper(I) complex with the ferrocene unit, [Cu(10)]BPh<sub>4</sub>, also reacted according to Eq. (1) and formed a quite stable peroxido complex at low temperatures. Stopped-flow measurements at  $-81$  °C are shown in Fig. 12 and nicely show the formation of this complex in the time resolved UV–vis spectra together with the decrease of the absorbance maxima of the superoxido complex at 410 nm (inset in Fig. 12).

### 3.4. Solid state reactions

As has been observed previously, by utilizing the anion tetraphenylborate, copper peroxido complexes with some tripodal ligands could be stabilized in the solid state to such an extent that it was possible to even heat them up to around a 100 °C and furthermore to use them for catalytic oxygenation of toluene [5,16]. To investigate the influence of the substitution at the terminal nitrogen atom, all solid copper(I) complexes with tetraphenylborate as anion were treated with dioxygen at room temperature. The results of the oxygen exposure of the complexes

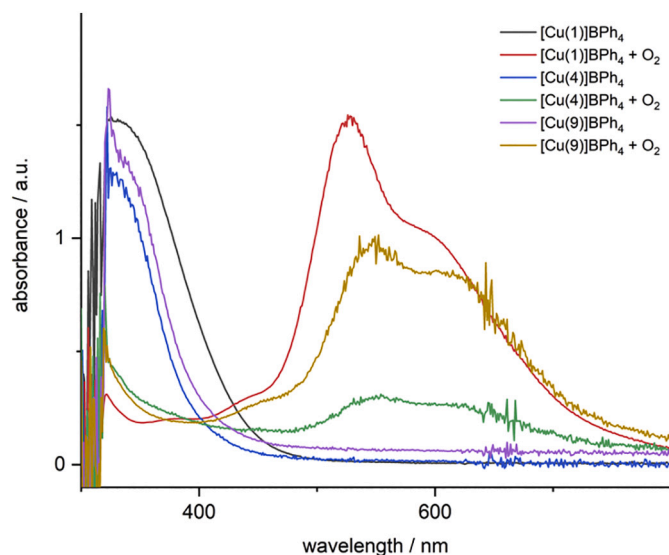


**Fig. 10.** UV–Vis of symmetric complexes [Cu(1)]BPh<sub>4</sub> and [Cu(4)]BPh<sub>4</sub> and the asymmetric complex [Cu(9)]BPh<sub>4</sub> in acetone at  $-85$  °C. Spectra are shown before and after treatment with dioxygen.

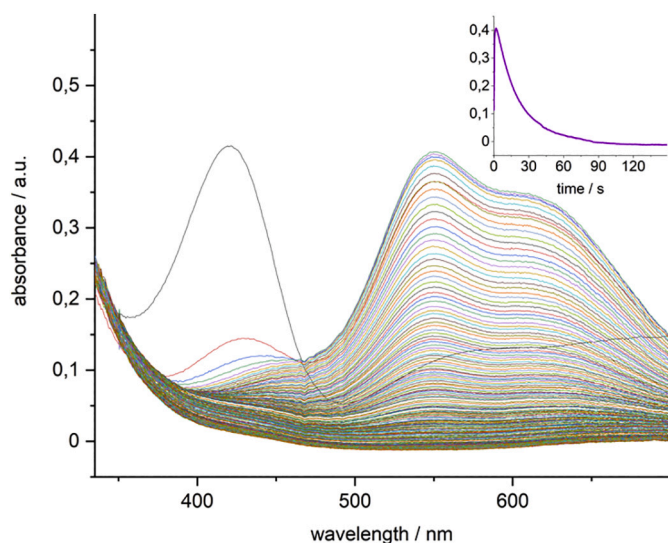


**Fig. 11.** Time-resolved spectra of the reaction of  $[\text{Cu}(4)]\text{BPh}_4$  with dioxygen in acetone at  $-83\text{ }^\circ\text{C}$  ( $[\text{complex}] = 2.0 \times 10^{-4}\text{ M}$ ,  $[\text{O}_2] = 4.4 \times 10^{-3}\text{ M}$ , total time: 150 s). At 420 nm the spectra shows the decreasing intensity of the superoxido intermediate. At 550 nm the increasing intensity of the labile peroxido complex is visible. The time trace at the upper right shows the fast decomposition of the peroxido species.

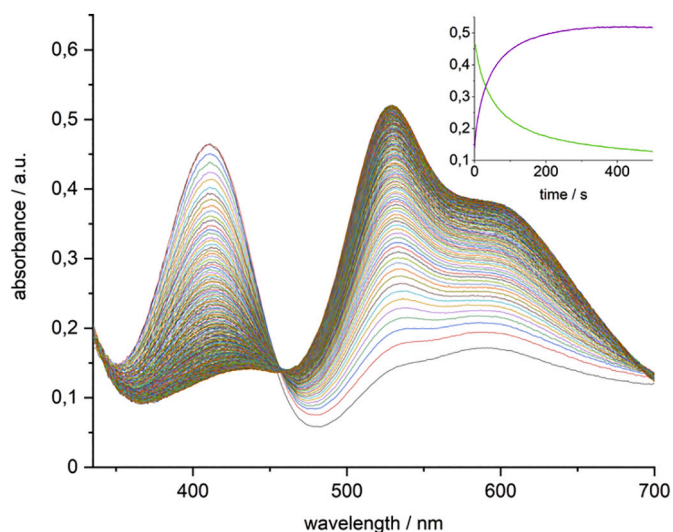


**Fig. 12.** Time-resolved spectra of the reaction of  $[\text{Cu}(10)]\text{BPh}_4$  with dioxygen in acetone at  $-81\text{ }^\circ\text{C}$  ( $[\text{complex}] = 2.0 \times 10^{-4}\text{ M}$ ,  $[\text{O}_2] = 4.4 \times 10^{-3}\text{ M}$ , total time: 500 s). At 410 nm the spectra show the decreasing intensity of the superoxido intermediate. At 528 nm the increasing intensity of the final peroxido complex is visible. The time trace at the upper right shows the formation of the peroxido species with the parallel decomposition of the superoxido complex.

with symmetric uns-penp derivatives are shown in Fig. 13, the results with the asymmetric ligands in Fig. 14.

As was observed previously, the yellow colored powder of  $[\text{Cu}(1)]\text{BPh}_4$  turned slowly into the intensively purple colored peroxido complex (Fig. 13 a) when reacted with dioxygen [5,16]. A diffuse reflectance UV-vis spectrum of the peroxido complex  $[(1)\text{CuO}_2\text{Cu}(1)](\text{BPh}_4)_2$  is reported in the Supporting Information (Fig. SI-4). In contrast no reaction was observed for complexes with ligands 2, 3 and 4. Furthermore, solid  $[\text{Cu}(10)]\text{BPh}_4$  did not react with dioxygen under these conditions (not shown in the pictures).

In contrast all solid copper(I) complexes with asymmetric ligands

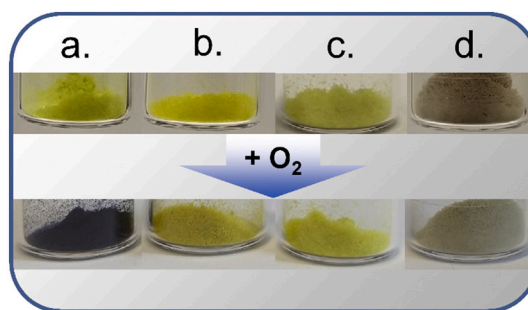


**Fig. 13.** Solid copper(I) complexes with symmetric uns-penp ligands after exposure with dioxygen; (a)  $[\text{Cu}(1)]\text{BPh}_4$ ; (b)  $[\text{Cu}(2)]\text{BPh}_4$ ; (c)  $[\text{Cu}(3)]\text{BPh}_4$ ; (d)  $[\text{Cu}(4)]\text{BPh}_4$ .

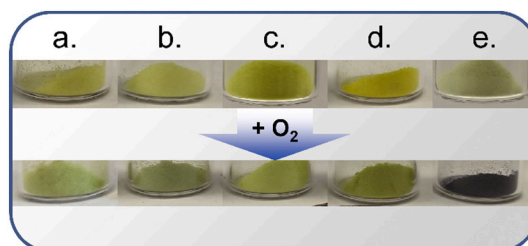


**Fig. 14.** Solid copper(I) complexes with asymmetric uns-penp ligands after exposure with dioxygen; (a)  $[\text{Cu}(5)]\text{BPh}_4$ ; (b)  $[\text{Cu}(6)]\text{BPh}_4$ ; (c)  $[\text{Cu}(7)]\text{BPh}_4$ ; (d)  $[\text{Cu}(8)]\text{BPh}_4$ ; (e)  $[\text{Cu}(9)]\text{BPh}_4$ .  $[\text{Cu}(10)]\text{BPh}_4$  did not show any reactivity in the solid state and was not considered.

5–9 exhibited a visible reaction with dioxygen. The yellow solids shown in Fig. 14 a-d reacted to a green solid (a bit difficult to see in the picture but very clear in the direct observation in the experiment). It is noticeable that these products kept their color and no further reaction to a purple/blue peroxido complex was observed. Reactions with the comparable complexes with tmpa and  $\text{Me}_2\text{uns-penp}$  also develop a green color shortly after exposure to dioxygen, which however, after some time, changed to a dark blue/purple color typical for a binuclear peroxido complex. The green color meanwhile is a hint for copper  $\eta^1$ -superoxido complex which is formed in a reversible reaction and is stable at room temperature [12,13,39,40]. Storing the  $[\text{Cu}(6)]\text{BPh}_4$  complex under argon atmosphere for a couple of days brought back the former yellow color. Treating the sample with oxygen led to the green colored compound again. Same results were obtained by heating the green solid up to  $50\text{ }^\circ\text{C}$  under an argon atmosphere. This effect was described previously by us within an investigation of the immobilization of copper complexes (with ligands derived from uns-penp) on silica surfaces [16].

$[\text{Cu}(9)]\text{BPh}_4$  (Fig. 14e) showed a different behavior, similar to the symmetric system with  $\text{Me}_2\text{uns-penp}$ . Here as well a binuclear peroxido complex was formed. Solid UV-Vis measurements supported this observation (see Supporting Information Fig. SI-4). But the formation works much faster than in the symmetric system. The first contact with dioxygen led immediately to the shown blue/purple color (video of this reaction is provided in the Supporting Information).

These results initiated a closer investigation to elucidate the differences between the symmetric and the asymmetric derivatizations of the ligands. Therefore the compounds  $[\text{Cu}(1)]\text{BPh}_4$ ,  $[\text{Cu}(3)]\text{BPh}_4$ ,  $[\text{Cu}(6)]\text{BPh}_4$  and  $[\text{Cu}(9)]\text{BPh}_4$  were investigated further.

Raman measurements of the oxygen treated copper(I) complexes are presented in Fig. 15. Especially the distinct band at  $830\text{ cm}^{-1}$  at the lower spectra of  $[\text{Cu}(1)]\text{BPh}_4$  demonstrates the formation of the trans- $\mu$ -1,2-peroxido complex [5]. Also the spectra of  $[\text{Cu}(9)]\text{BPh}_4$  contains this feature but with a relative small intensity. More striking is the presence of that band in the spectra of  $[\text{Cu}(6)]\text{BPh}_4$  which does not show

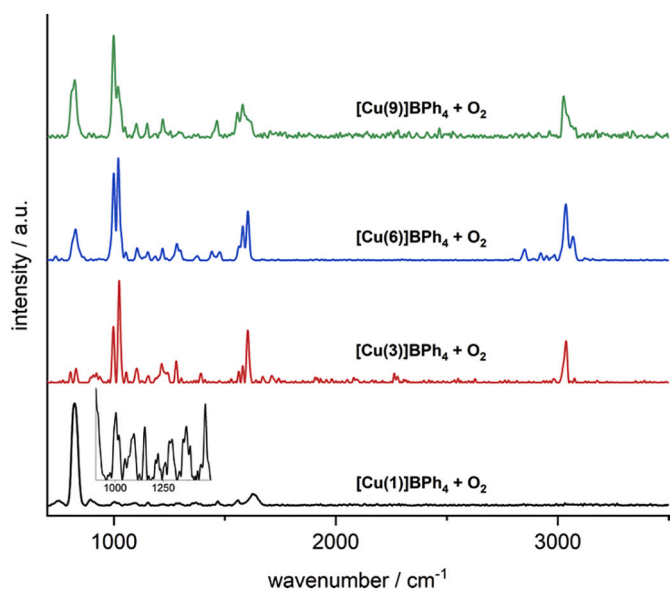


**Fig. 15.** Raman measurement of the complexes [Cu(1)]BPh<sub>4</sub>, [Cu(3)]BPh<sub>4</sub>, [Cu(6)]BPh<sub>4</sub> and [Cu(9)]BPh<sub>4</sub> after treatment with oxygen. The band around 830 cm<sup>-1</sup> indicates a peroxide species. The inset shows the spectrum of [Cu(1)]BPh<sub>4</sub> magnified between 900 and 1750 cm<sup>-1</sup>.

an obvious conversion into a blue product. An explanation for this finding might be that a small amount of the batch is converted to the peroxido complex which cannot be seen by looking at the sample. The spectrum of the [Cu(3)]BPh<sub>4</sub> complex did not show any sign of a reaction with dioxygen. This correlates with the visual findings. The absorbance around 1020 cm<sup>-1</sup> is common for all complexes investigated. It is assigned as a ring and C–H stretching mode of the coordinated pyridine residues [41]. The inset shows a magnified region in the spectrum of complex [Cu(1)]BPh<sub>4</sub>. Due to the strong resonance of the peroxido ligand the intensities of the remaining bands almost disappear. Only by magnification at the corresponding wavelengths made visible.

To gain information about the change in the crystal structure of the solid compounds, powder XRD measurements under inert conditions before and after exposure with dioxygen were performed. Recorded diffractograms of [Cu(3)]BPh<sub>4</sub>, [Cu(6)]BPh<sub>4</sub> and [Cu(9)]BPh<sub>4</sub> compared with the corresponding diffraction patterns of the educts of the complex synthesis simulated from single crystal data are given in the Supporting Information (Fig. SI-5 – SI-7) to verify phase purity.

The diffractograms of the complex [Cu(1)]BPh<sub>4</sub> before and after the treatment with dioxygen as well as a comparison with a simulated pattern from single crystal data as well as patterns of the reagents are shown in Fig. 16. Small deviations of the simulated from the experimental diffraction pattern can be explained by different measurement temperatures of single crystal XRD and powder XRD. By comparing the patterns before and after the treatment with dioxygen, it is obvious that [Cu(1)]BPh<sub>4</sub> undergoes a transformation upon exposure to dioxygen, as the PXRD after the treatment strongly differs from the pattern before and also does not coincide with the simulated pattern anymore.

The results of the powder XRD measurements of [Cu(3)]BPh<sub>4</sub> with the symmetric ligand Prop<sub>2</sub>uns-penp are shown in Fig. SI-5. Comparing the simulated diffraction pattern of [Cu(3)]BPh<sub>4</sub> (black) with the recorded pattern (red), a slight shift of the reflections of the experimental diffractogram towards higher angles in 2θ can be noticed due to the different temperatures. Different to [Cu(1)]BPh<sub>4</sub>, a comparison of the experimental powder diffraction patterns before and after dioxygen exposure reveals good accordance for [Cu(3)]BPh<sub>4</sub>. This indicates that the lattice parameters do not differ significantly. In combination with the findings of Figs. 13 and 15, a reaction with oxygen seems to be unlikely.

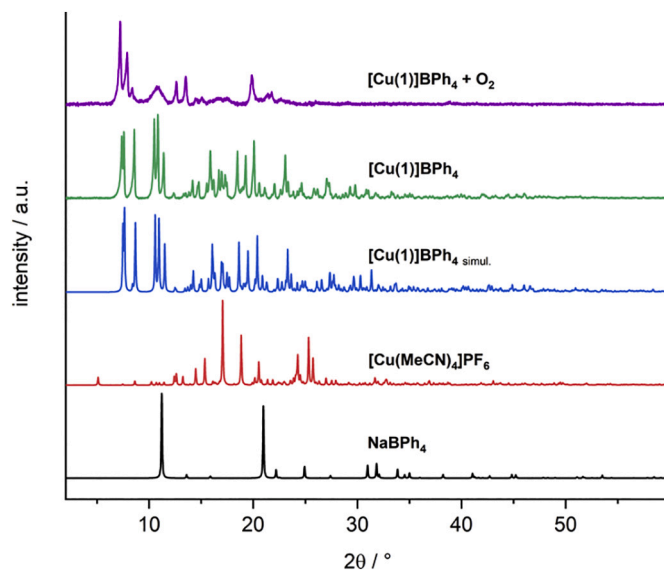


**Fig. 16.** Powder XRD patterns of [Cu(1)]BPh<sub>4</sub> measured before (green) and after the treatment with dioxygen (purple) in comparison to powder diffraction patterns of [Cu(1)]BPh<sub>4</sub> simulated from single crystal data (blue), NaBPh<sub>4</sub> (black) [42], and [Cu(MeCN)<sub>4</sub>]PF<sub>6</sub> (red) [43]. (For interpretation of the references to color in this figure legend, the reader is referred to the web version of this article.)

Comparable results were obtained from the investigation of the complex [Cu(6)]BPh<sub>4</sub> with the asymmetric ligand (see Supporting Information Fig. SI-6). Although there has been a change in color detected for the product, there is no observable change in the powder pattern and thus meaning no change in crystal structure and lattice. Due to these findings, an insertion of a dioxygen molecule would be unlikely, too, by means of the result of PXRD. Nonetheless, the single crystal measurement of [Cu(6)]BPh<sub>4</sub> indicates the structural possibility of a reaction with dioxygen. A change in color is observable upon dioxygen treatment, which indicates a suchlike insertion. A possible explanation for the discrepancy to powder XRD data is an insertion of dioxygen in low quantity only and not for the bulk material. Thus, in the measured powder diffraction pattern, only the majority phase is observable, which is the un-reacted complex [Cu(6)]BPh<sub>4</sub>, and still the color change can apply.

Quite surprisingly, the small crystals of [Cu(9)]BPh<sub>4</sub>, which were obtained by precipitation into diethylether during the common complexation and anion exchange reactions retain an adequate crystallinity after their reaction with dioxygen. The crystals were still suitable for single crystal X-ray analysis. Fig. 17 shows the molecular structure of the binuclear peroxido complex [(9)Cu(O<sub>2</sub>)Cu(9)](BPh<sub>4</sub>)<sub>2</sub> obtained this way. This complex is quite similar to the other three structurally characterized *end-on* peroxido copper complexes with the tripodal ligands tmpa, Bz<sub>3</sub>tren, Me<sub>6</sub>tren and a bit different to the copper complex with the macrocyclic ligand tet b [5,7,44,45]. Our previous efforts to accomplish the same solid state reaction with the copper Me<sub>6</sub>tren system had failed. After the reaction with dioxygen the complex had become amorphous and the peroxido complex had to be crystallized in a different way [5]. Crystallographic data of the complex [(9)Cu(O<sub>2</sub>)Cu(9)](BPh<sub>4</sub>)<sub>2</sub> are reported in the Supporting Information (Table SI-77-81).

Therefore, it was also possible to achieve the insertion of dioxygen into the bulk substance of [Cu(9)]BPh<sub>4</sub>. The experimental powder diffractograms of [Cu(9)]BPh<sub>4</sub> before and after dioxygen treatment in comparison to the powder diffraction patterns simulated from single crystal data are depicted in Fig. 18. In both cases, the measured diffraction patterns are in good accordance to the simulated patterns, indicating the structures, single crystal structure analysis as bulk products, too. However, there is a distinct change in structure detectable

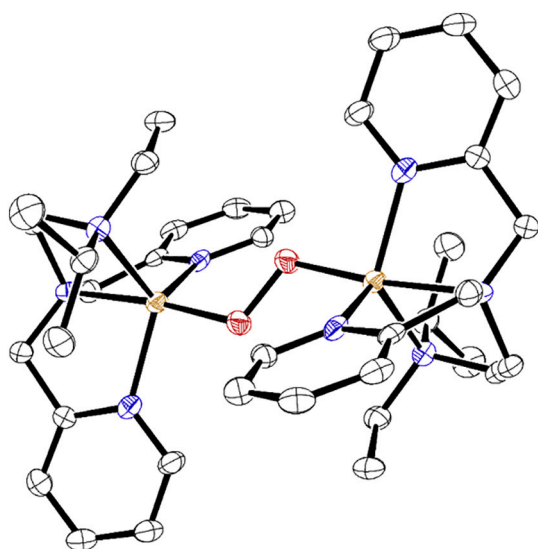


**Fig. 17.** Molecular structure of the cation of binuclear  $[(9)\text{Cu}(\text{O}_2)\text{Cu}(9)](\text{BPh}_4)_2$ . Ellipsoids set at 50% probability; the anions, H atoms, and solvent molecules are omitted for clarity. Carbon: black; nitrogen: blue; oxygen: red; copper: brown. (For interpretation of the references to color in this figure legend, the reader is referred to the web version of this article.)

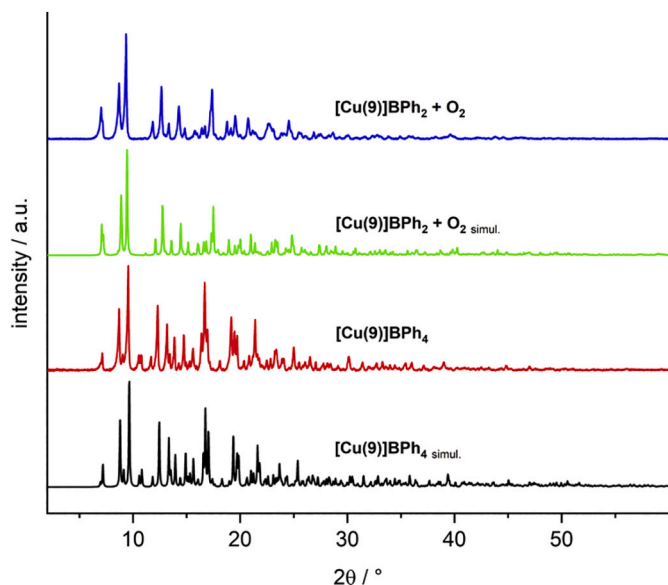


**Fig. 18.** Powder XRD patterns for  $[\text{Cu}(9)]\text{BPh}_4$  before (red) and after the treatment with dioxygen (blue) compared with the powder diffraction patterns of  $[\text{Cu}(9)]\text{BPh}_4$  and  $[\text{Cu}(9)\text{O}_2](\text{BPh}_4)_2$  simulated from single crystal data (black). (For interpretation of the references to color in this figure legend, the reader is referred to the web version of this article.)

upon dioxygen treatment, as it can be seen by differences in number, intensities and positions of reflections between initial and  $[\text{Cu}(9)]\text{BPh}_4$  flushed with dioxygen. In contrast to the proposed reactivity towards dioxygen of complex  $[\text{Cu}(6)]\text{BPh}_4$ , a complete conversion of  $[\text{Cu}(9)]\text{BPh}_4$  to the oxygenated product  $[\text{Cu}(9)\text{O}_2](\text{BPh}_4)_2$  can be observed corroborated by comparison of simulated with experimental patterns.

**Table 2** contains the values of the unit cells before and after exposure to oxygen. Comparison of the unit cells reveals only a slight expansion of the unit cell of the peroxido complex. The relative change is less than 2%.

Furthermore, there is a small deformation between two and three

**Table 2**

Cell parameters received from single crystal data of  $[\text{Cu}(9)]\text{BPh}_4$  complex before and after oxygenation.

$[\text{Cu}(9)]\text{BPh}_4$			
a / Å	11.3474(19)	$\alpha$ / °	94.310(5)
b / Å	13.161(2)	$\beta$ / °	111.929(5)
c / Å	13.443(2)	$\gamma$ / °	101.989(6)
$[\text{Cu}(9)\text{O}_2](\text{BPh}_4)_2$			
a / Å	11.392(3)	$\alpha$ / °	97.027(7)
b / Å	12.911(3)	$\beta$ / °	109.247(7)
c / Å	13.538(3)	$\gamma$ / °	103.938(7)
Relative differences			
a / %	0.39%	$\alpha$ / %	2.80%
b / %	1.94%	$\beta$ / %	2.45%
c / %	0.70%	$\gamma$ / %	1.88%

degrees detectable. The complete structural parameters for the crystal structure are reported in the Supporting Information. This single crystal to single crystal transformation is most likely made possible due to the orientation of the copper center towards its symmetry equivalent in the crystal structure. Two copper ions are directly facing each other (**Fig. 5**). The distance between them decreases after the formation of the peroxido complex (5.591 Å to 4.475 Å), however, the relative orientation almost remains. This special geometry is not observed in the complexes with the other ligand derivatives. The metal centers in the crystal lattice of e. g.  $[\text{Cu}(1)]\text{BPh}_4$  are orientated adversely towards each other (**Fig. 4**). The copper-copper distance is 12.230 Å. An *end-on* peroxide formation will therefore lead to a complete loss of crystallinity.

#### 4. Conclusion

Investigations on the reactivity of a series of copper(I) complexes  $[\text{Cu}(\text{L})]\text{BPh}_4$  towards dioxygen were performed to gain a better understanding of the steric influence of a tripodal ligand system. The ligand L,  $\text{R}^1\text{-R}^2\text{-uns-penp}$  (uns-penp = (2-aminoethyl)bis(2-pyridylmethyl) amine), was chosen because, while the bispicolylamine unit already stabilized the copper(I) unit, the additional amine arm could be easily modified. In combination with the same anion (tetraphenylborate is essential for stabilization of the complexes in the solid state) it could be shown that the redox potential  $\text{Cu}(\text{I})/\text{Cu}(\text{II})$  for nearly all complexes was quite similar. Therefore, only the different alkyl groups bound to the amine arm were responsible for different reactivities. While  $\text{Me}_2\text{uns-penp}$  as a ligand still supported quite slow formation of a solid peroxido complex, symmetric substitution with two ethyl, propyl or isopropyl groups completely suppressed reactivity of the corresponding copper(I) complexes (in the solid state) towards dioxygen. Quite surprisingly, however, was the observation that copper(I) complexes with ligands with asymmetric substitution of the amine nitrogen,  $\text{Me-Et-uns-penp}$  (**5**),  $\text{Me-Prop-uns-penp}$  (**6**),  $\text{Et-Prop-uns-penp}$  (**7**),  $\text{Me-iProp-uns-penp}$  (**8**) and  $\text{Et-iProp-uns-penp}$  (**9**) clearly showed reactivity towards dioxygen in the solid state. Copper(I) complexes with ligands **5–8** reversibly formed a green compound that indicated formation of a mononuclear superoxido complex, however, so far and as described previously, we did not find a way to really characterize these products [16]. In contrast,  $[\text{Cu}(9)]\text{BPh}_4$  instantly reacted with dioxygen to form a stable *trans-μ-1,2-peroxido* product complex that could be structurally characterized. A look at the crystal structures of the copper(I) complexes of all ligands clearly showed that  $[\text{Cu}(9)]\text{BPh}_4$  is kind of preformed for the uptake of dioxygen and only has to undergo minor changes in the overall geometry when reacted to the copper(II) peroxido complex. Usually copper(I) complexes undergo a big change in coordination geometry/coordination number (bond lengths and angles) when oxidized to the corresponding copper(II) complexes. However, this is slightly different for copper complexes with tripodal ligands and thus allowed with the modification of the uns-penp ligand to find a perfect system for the fast uptake of dioxygen without a major structure change. Definitely

we could prove that slight modifications of the tripodal ligand system can have a large effect on the chemistry of the corresponding copper complexes.

### Declaration of Competing Interest

The authors declare that they have no known competing financial interests or personal relationships that could have appeared to influence the work reported in this paper.

### Acknowledgements

Prof. Dr. Roland Marschall (Fakultät für Biologie, Chemie und Geowissenschaften, Universität Bayreuth) is acknowledged for his support of the solid-state UV–vis measurements.

### Appendix A. Supplementary data

Supplementary data to this article can be found online at <https://doi.org/10.1016/j.jinorgbio.2021.111544>.

### References

- [1] E.I. Solomon, D.E. Heppner, E.M. Johnston, J.W. Ginsbach, J. Cirera, M. Qayyum, M.T. Kieber-Emmons, C.H. Kjaergaard, R.G. Hadt, L. Tian, Copper active sites in biology, *Chem. Rev.* 114 (2014) 3659–3853, <https://doi.org/10.1021/cr400327t>.
- [2] D.A. Quist, D.E. Diaz, J.J. Liu, K.D. Karlin, Activation of dioxygen by copper metalloproteins and insights from model complexes, *J. Biol. Inorg. Chem.* 22 (2017) 253–288, <https://doi.org/10.1007/s00775-016-1415-2>.
- [3] S. Herres-Pawlis, P. Verma, R. Haase, P. Kang, C.T. Lyons, E.C. Wasinger, U. Florke, G. Henkel, T.D.P. Stack, Phenolate hydroxylation in a bis( $\mu$ -oxo)dicopper(III) complex: lessons from the guanidine/amine series, *J. Am. Chem. Soc.* 131 (2009) 1154–1169, <https://doi.org/10.1021/ja807809x>.
- [4] A. Hoffmann, C. Citek, S. Binder, A. Goos, M. Rübhausen, O. Troepfner, I. Ivanović-Burmazović, E.C. Wasinger, T.D.P. Stack, S. Herres-Pawlis, Catalytic Phenol hydroxylation with dioxygen: extension of the tyrosinase mechanism beyond the protein matrix, *Angew. Chemie - Int. Ed.* 52 (2013) 5398–5401, <https://doi.org/10.1002/anie.201301249>.
- [5] C. Würtele, O. Sander, V. Lutz, T. Waitz, F. Tuczek, S. Schindler, Aliphatic C-H bond oxidation of toluene using copper peroxo complexes that are stable at room temperature, *J. Am. Chem. Soc.* 131 (2009) 7544–7545, <https://doi.org/10.1021/ja902327s>.
- [6] H.R. Lucas, L. Li, A.A.N. Sarjeant, M.A. Vance, E.I. Solomon, K.D. Karlin, Toluene and ethylbenzene aliphatic C-H bond oxidations initiated by a Dicopper(II)- $\mu$ -1,2-peroxo complex, *J. Am. Chem. Soc.* 131 (2009) 3230–3245, <https://doi.org/10.1021/ja907081d>.
- [7] R.R. Jacobson, Z. Tyecklar, A. Farooq, K.D. Karlin, S. Liu, J. Zubieta, A Cu<sub>2</sub>–O<sub>2</sub> complex. Crystal structure and characterization of a reversible dioxygen binding system, *J. Am. Chem. Soc.* 110 (1988) 3690–3692, <https://doi.org/10.1021/ja00219a071>.
- [8] S. Kaderli, N. Wei, K.D. Karlin, B. Jung, A.D. Zuberbühler, P. Niklaus, Kinetics and thermodynamics of formation of copper-Dioxygen adducts: oxygenation of mononuclear copper(I) complexes containing Tripodal Tetradentate ligands, *J. Am. Chem. Soc.* 115 (1993) 9506–9514, <https://doi.org/10.1021/ja00074a015>.
- [9] C.X. Zhang, S. Kaderli, M. Costas, E. Il Kim, Y.M. Neuhold, K.D. Karlin, A. D. Zuberbühler, Copper(I)–dioxygen reactivity of [(L)Cu]+ (L) Tris(2-pyridylmethyl)amine: kinetic/thermodynamic and spectroscopic studies concerning the formation of Cu–O<sub>2</sub> and Cu<sub>2</sub>–O<sub>2</sub> adducts as a function of solvent medium and 4-pyridyl ligand substituent variations, *Inorg. Chem.* 42 (2003) 1807–1824, <https://doi.org/10.1021/ic0205684>.
- [10] M. Weitzer, S. Schindler, G. Brehm, S. Schneider, E. Hörmann, B. Jung, S. Kaderli, A.D. Zuberbühler, Reversible binding of dioxygen by the copper(I) complex with Tris(2-dimethylaminoethyl)amine (Me<sub>6</sub>tren) ligand, *Inorg. Chem.* 42 (2003) 1800–1806, <https://doi.org/10.1021/ic025941m>.
- [11] J. Will, C. Würtele, J. Becker, O. Walter, S. Schindler, Synthesis, crystal structures and reactivity towards dioxygen of copper(I) complexes with tripodal aliphatic amine ligands, *Polyhedron*. 171 (2019) 448–454, <https://doi.org/10.1016/j.poly.2019.07.007>.
- [12] C. Würtele, E. Gaoutchenova, K. Harms, M.C. Holthausen, J. Sundermeyer, S. Schindler, Crystallographic characterization of a synthetic 1:1 end-on copper dioxygen adduct complex, *Angew. Chem. Int. Ed.* 45 (2006) 3867–3869, <https://doi.org/10.1002/anie.200600351>.
- [13] M. Schatz, V. Raab, S.P. Foxon, G. Brehm, S. Schneider, M. Reiher, M. C. Holthausen, J. Sundermeyer, S. Schindler, Combined spectroscopic and theoretical evidence for a persistent end-on copper Superoxo complex, *Angew. Chem. Int. Ed.* 43 (2004) 4360–4363, <https://doi.org/10.1002/anie.200454125>.
- [14] T. Hoppe, P. Josephs, N. Kempf, C. Wölper, S. Schindler, A. Neuba, G. Henkel, An approach to model the active site of Peptidylglycine- $\alpha$ -hydroxylating monooxygenase (PHM), *Z. Anorg. Allg. Chem.* 639 (2013) 1504–1511, <https://doi.org/10.1002/zaac.201300066>.
- [15] M. Bhadra, W.J. Transue, H. Lim, R.E. Cowley, J.Y.C. Lee, M.A. Siegler, P. Josephs, G. Henkel, M. Lerch, S. Schindler, A. Neuba, K.O. Hodgson, B. Hedman, E. I. Solomon, K.D. Karlin, A Thioether-ligated cupric superoxide model with hydrogen atom abstraction reactivity, *J. Am. Chem. Soc.* 143 (2021) 3707–3713, <https://doi.org/10.1021/jacs.1c00260>.
- [16] T. Brückmann, J. Becker, K. Turke, B. Smarsly, M. Weiß, R. Marschall, S. Schindler, Immobilization of a copper complex based on the tripodal ligand (2-aminoethyl)bis(2-pyridylmethyl)amine (uns-penp), *Z. Anorg. Allg. Chem.* 647 (2021) 560–571, <https://doi.org/10.1002/zaac.202100022>.
- [17] G.J. Kubas, B. Monzyk, A.L. Crumbliss, Tetrakis(acetonitrile)copper(I) Hexafluorophosphate, *Inorg. Synth.* 19 (1979) 90–92, <https://doi.org/10.1002/9780470132500.ch18>.
- [18] J.W. Gooch, Kubelka-Munk equation, in: J.W. Gooch (Ed.), *Encycl. Dict. Polym.*, Springer Verlag, New York, NY, 2007, pp. 559–560, [https://doi.org/10.1007/978-0-387-30160-0\\_6609](https://doi.org/10.1007/978-0-387-30160-0_6609).
- [19] M. Weitzer, M. Schatz, F. Hampel, F.W. Heinemann, S. Schindler, Low temperature stopped-flow studies in inorganic chemistry, *Dalton Trans.* (2002) 686–694, <https://doi.org/10.1039/b107927c>.
- [20] S.V. Kryatov, E.V. Rybak-Akimova, S. Schindler, Kinetics and mechanisms of formation and reactivity of non-heme Iron oxygen intermediates, *Chem. Rev.* 105 (2005) 2175–2226, <https://doi.org/10.1021/cr030709z>.
- [21] N. Elgrishi, K.J. Rountree, B.D. McCarthy, E.S. Rountree, T.T. Eisenhart, J. L. Dempsey, A practical Beginner's guide to cyclic voltammetry, *J. Chem. Educ.* 95 (2018) 197–206, <https://doi.org/10.1021/acs.jchemed.7b00361>.
- [22] C. Komiya, K. Aihara, K. Morishita, H. Ding, T. Inokuma, A. Shigenaga, A. Otaka, Development of an Intein-inspired amide cleavage chemical device, *J. Organomet. Chem.* 81 (2016) 699–707, <https://doi.org/10.1021/acs.joc.5b02399>.
- [23] M. Schatz, M. Leibold, S.P. Foxon, M. Weitzer, F.W. Heinemann, F. Hampel, O. Walter, S. Schindler, Synthesis and characterization of copper complexes of the ligand (2-aminoethyl)bis(2-pyridylmethyl)amine (uns-penp) and derivatives, *Dalton Trans.* (2003) 1480–1487.
- [24] G.J.P. Britovsek, J. England, A.J.P. White, Non-heme Iron(II) complexes containing tripodal tetradentate nitrogen ligands and their application in alkane oxidation catalysis, *Inorg. Chem.* 44 (2005) 8125–8134, <https://doi.org/10.1021/ic0509229>.
- [25] M. Balamurugan, R. Mayilmurugan, E. Suresh, M. Palaniandavar, Nickel(II) complexes of tripodal 4N ligands as catalysts for alkane oxidation using m-CPBA as oxidant: ligand stereoelectronic effects on catalysis, *Dalton Trans.* 40 (2011) 9413–9424, <https://doi.org/10.1039/c1dt10902b>.
- [26] C. Suspène, S. Brandès, R. Guillard, Reversible coordination of Dioxygen by Tripodal Tetraamine copper complexes incorporated in a porous silica framework, *Chem. Eur. J.* 16 (2010) 6352–6364, <https://doi.org/10.1002/chem.200903148>.
- [27] C. Würtele, End-On “Copper Dioxygen Adduct Complexes” PhD thesis. <http://web.uni-giessen.de/geb/volltexte/2008/6469/pdf/WuerteleChristian-2008-09-26.pdf>, 2008.
- [28] M. Schatz, M. Becker, F. Thaler, F. Hampel, S. Schindler, R.R. Jacobson, Z. Tyecklar, N.N. Murthy, P. Ghosh, Q. Chen, J. Zubieta, K.D. Karlin, Copper(I) complexes, copper(I)/O<sub>2</sub> reactivity, and copper(II) complex adducts, with a series of tetradentate tripyridylalkylamine tripodal ligands, *Inorg. Chem.* 40 (2001) 2312–2322, <https://doi.org/10.1021/ic000924n>.
- [29] M. Becker, F.W. Heinemann, S. Schindler, Reversible binding of dioxygen by a copper (I) complex with Tris (2-dimethylaminoethyl) amine (Me<sub>6</sub>tren) as a ligand, *Chem. Eur. J.* 5 (1999) 3124–3129, <https://doi.org/10.1021/ic025941m>.
- [30] D. Maiti, J.S. Woertink, A.A.N. Sarjeant, E.I. Solomon, K.D. Karlin, Copper dioxygen adducts: formation of Bis( $\mu$ -oxo)dioxygen(III) versus ( $\mu$ -1,2) Peroxodicopper(II) complexes with small changes in one Pyridyl-ligand substituent, *Inorg. Chem.* 47 (2008) 3787–3800, <https://doi.org/10.1021/ic702437c>.
- [31] J.V. Folgado, E. Coronado, D. Beltrán-Porter, R. Burriel, A. Fuertes, C. Miravittles, Crystal structures and magnetic properties of the mono- $\mu$ -halogeno-bridged copper (II) chains Cu<sub>2</sub>(pccp)X [pccp = N-(2'-pyridylcarbonyl)pyridine-2- carboximidate, X = Cl or Br], *J. Chem. Soc. Dalton Trans.* (1988) 3041–3045, <https://doi.org/10.1039/DT9880003041>.
- [32] K. Abdi, H. Hadadzadeh, M. Weil, H.A. Rudbari, Mono- and polynuclear copper(II) complexes based on 2,4,6-tris(2-pyridyl)- 1,3,5-triazine and its hydrolyzed form, *Inorg. Chim. Acta* 416 (2014) 109–121, <https://doi.org/10.1016/j.ica.2014.03.021>.
- [33] M. Schatz, M. Becker, O. Walter, G. Liehr, S. Schindler, Reactivity towards dioxygen of a copper(I) complex of tris(2-benzylaminoethyl)amine, *Inorg. Chim. Acta* 324 (2001) 173–179, [https://doi.org/10.1016/S0020-1693\(01\)00588-6](https://doi.org/10.1016/S0020-1693(01)00588-6).
- [34] T.D.J. Stumpf, M. Steinbach, C. Würtele, J. Becker, S. Becker, R. Fröhlich, R. Göttlich, S. Schindler, Reactivity of copper complexes with Bis(piperidiny) methane and Bis(quinolinyl)methane ligands, *Eur. J. Inorg. Chem.* (2017) 4246–4258, <https://doi.org/10.1002/ejic.201700755>.
- [35] A.A.O. Sarhan, M.S. Ibrahim, M.M. Kamal, K. Mitobe, T. Izumi, Synthesis, cyclic voltammetry, and UV-Vis studies of ferrocene- dithiafulvalenes as anticipated electron-donor materials, *Monatsh. Chem.* 140 (2009) 315–323, <https://doi.org/10.1007/s00706-008-0025-2>.
- [36] S. Schindler, Reactivity of copper(I) complexes towards Dioxygen, *Eur. J. Inorg. Chem.* (2000) 2311–2326, [https://doi.org/10.1002/1099-0682\(200011\)2000:11<2311::aid-ejic2311>3.0.co;2-7](https://doi.org/10.1002/1099-0682(200011)2000:11<2311::aid-ejic2311>3.0.co;2-7).
- [37] E.E. Elwell, N.L. Gagnon, B.D. Neisen, D. Dhar, A.D. Spaeth, G.M. Yee, W. B. Tolman, Copper-oxygen complexes revisited: structures, spectroscopy, and

- reactivity, *Chem. Rev.* 117 (2017) 2059–2107, <https://doi.org/10.1021/acs.chemrev.6b00636>.
- [38] L.M. Mirica, X. Ottenwaelder, T.D.P. Stack, Structure and spectroscopy of copper-dioxygen complexes, *Chem. Rev.* 104 (2004) 1013–1045, <https://doi.org/10.1021/cr020632z>.
- [39] D. Maiti, D.-H. Lee, K. Gaoutchenova, C. Würtele, M.C. Holthausen, A.A. Narducci Sarjeant, J. Sundermeyer, S. Schindler, K.D. Karlin, Reactions of a copper(II) superoxo complex Lead to C-H and O-H substrate oxygenation: modeling copper-monoxygenase C-H hydroxylation, *Angew. Chem.* 120 (2008) 88–91, <https://doi.org/10.1002/ange.200704389>.
- [40] S. Itoh, Developing mononuclear copper-active-oxygen complexes relevant to reactive intermediates of biological oxidation reactions, *Acc. Chem. Res.* 48 (2015) 2066–2074, <https://doi.org/10.1021/acs.accounts.5b00140>.
- [41] G. Socrates, *Infrared and Raman Characteristic Group Frequencies. Tables and Charts Vol.3*, J. Wiley and Sons, Chichester, 2001.
- [42] A.Y. Kovalevsky, P. Coppens, CSD Communications, CSD Commun, 1999, <https://doi.org/10.5517/cc4l24x>.
- [43] L.A. Dakin, P.C. Ong, J.S. Panek, R.J. Staples, P. Stavropoulos, Speciation and mechanistic studies of chiral copper(I) Schiff Base precursors mediating asymmetric Carbenoid insertion reactions of Diazoacetates into the Si-H bond of Silanes, *Organometallics*. 19 (2000) 2896–2908, <https://doi.org/10.1021/om0003786>.
- [44] S. Fujinami, A. Hashimoto, K. Komiyama, S. Nagatomo, T. Kitagawa, M. Suzuki, H. Hayashi, H. Furutachi, Dioxygen reactivity of copper(I) complexes with Tetradentate Tripodal ligands having aliphatic nitrogen donors: synthesis, structures, and properties of Peroxo and Superoxo complexes, *Bull. Chem. Soc. Jpn.* 77 (2004) 59–72, <https://doi.org/10.1246/bcsj.77.59>.
- [45] T. Hoppe, S. Schaub, J. Becker, C. Würtele, S. Schindler, Charakterisierung eines makrocyclischen “end-on”-Peroxidokupferkomplexes, *Angew. Chem.* 125 (2013) 904–907, <https://doi.org/10.1002/ange.201205663>.